Use of a Paramagnetic Core to Affect Longitudinal Nuclear Relaxation in Dendrimers—A Tool for Probing Dendrimer Conformation

Christopher B. Gorman,* Michael W. Hager, Brandon L. Parkhurst, and Jennifer C. Smith

Box 8204, Department of Chemistry, North Carolina State University, Raleigh, North Carolina 27695

Received October 10, 1997; Revised Manuscript Received December 5, 1997

ABSTRACT: The longitudinal relaxation time constants (T_1) of the protons in a series of dendrimers that alternatively had paramagnetic ($[Fe_4S_4(SR)_4]^{2-}$, R = dendron) and diamagnetic (tetraphenylmethane) cores were compared. The T_1 values of the phenyl and benzyl protons in the paramagnetic core dendrimers were attenuated compared to those of analogous protons in the diamagnetic core dendrimers. This observation indicated that protons in each set of topologically different repeat units (generation) of the dendrimer approach the core of the molecule closely in space. This conclusion is consistent with the computed radial density distributions of the different generations calculated from molecular dynamics simulations. In addition, by comparing T_1 values of protons at two slightly different temperatures, the terminal groups in both sets of dendrimers were concluded to be, on average, more mobile than the other generations within the dendrimers. This conclusion is consistent with the computed mean square displacement correlation functions for the different generations also calculated from molecular dynamics simulations.

Introduction

Probing the conformation of dendrimers in various environments is an important step in understanding and predicting their behavior. Several demonstrations have suggested uses for dendrimers in such areas as molecular recognition,[1−3] surface modification,[4−7] asymmetric synthesis,[8,9] and small-molecule encapsulation.[10,11] To develop structure−property relationships for dendrimer conformation and to engage in rational design strategies for new dendrimeric structures, several methods for probing conformation have emerged. These include the study of their viscosity behavior[12−14] and the use of solvatochromic,[15] electrochemical,[16,17] photochemical,[18−20] nuclear magnetic resonance,[10,20−22] and electron paramagnetic resonance[23−25] probes.

Recently, we reported the synthesis, characterization, and electrochemical behavior of a series of iron−sulfur core dendrimers of the form $(n\text{Bu}_4\text{N})_2[Fe_4S_4(\text{S-Dend})_4]$.[26] Iron−sulfur clusters are ubiquitous in nature where they function as electron transfer and storage sites as well as active sites and structure-enforcing units in enzymes.[27−29] The $Fe_4S_4(SR)_4^{2-}$ moiety has also been the subject of several model studies that helped to define its reactivity and electrochemical and magnetic behavior.[30−34] Inorganic cluster cores can be used to prepare highly symmetrical dendrimers as well as dendrimers with electroactive, luminescent, and/or paramagnetic centers.[26]

It is this latter property that is the subject of this paper. Iron−sulfur clusters containing the $[Fe_4S_4(SR)_4]^{2-}$ (R = heretofore a small alkyl or aryl group) moiety are paramagnetic with a magnetic moment of approximately 2 μ_B at room temperature.[27,35] Previously, we noted that this core results in small Fermi contact shifts and line broadening of the ^{1}H NMR signals of protons a few bonds away from it.[26,33] This feature was utilized as spectroscopic evidence for the formation of iron−sulfur core dendrimers. The paramagnetic core of the molecule can also influence the longitudinal relaxation time constants (T_1) of nuclei in the dendrimer.

In this paper, a paramagnetic core $Fe_4S_4(SR)_4^{2-}$ was used to probe the average proximity of nuclei in the dendrimer with respect to the molecular core. By comparing the longitudinal relaxation time constants (T_1) of structurally similar dendrimers in which the core is alternatively paramagnetic and diamagnetic, the relative contribution of the paramagnetic center to the overall relaxation was determined. For paramagnetic relaxation to make a contribution to T_1, the nuclei must be in close proximity to the core (the efficiency of relaxation will decay as $1/r^6$, where r is the distance between nucleus and core). Reduction of T_1 was observed, indicating some close approach of each part of the molecule to the core. These observations support a model of dendrimer conformation for dendrimers up to generation 3 containing floppy subunits in which all of the different generations within a dendrimer are radially distributed throughout it and do not exist in a "shell-like" conformation with respect to the center of the molecule.

NMR techniques have been used previously to probe dendrimer and dendron (e.g. a structure composed of one arm of a dendrimer) conformation, respectively. Meltzer et al.[36,37] employed ^{13}C NMR to probe relaxation in PAMAM type dendrimers, but only the terminal and internal nuclei were chemical shift distinguishable in this case. In the work reported here, the chemical shifts of the protons in all different generations of each molecule are distinguishable. Wooley et al.[38] employed REDOR NMR on dendrons in the solid state and came to the conclusion that the terminal generations (e.g. those at the topological periphery) of a nuclear-spin-labeled dendron were found to come into close contact with a differently nuclear-spin-labeled focal point. Although the dendrons in this study[38] and the dendrimers reported here had similar molecular weights, these two types of molecules are topologically very different.

Results and Discussion

A. Dendrimer Synthesis and Characterization. The molecules under study are shown in Figure 1.

S0024-9297(97)01497-6 CCC: $15.00
Published on Web 01/23/1998

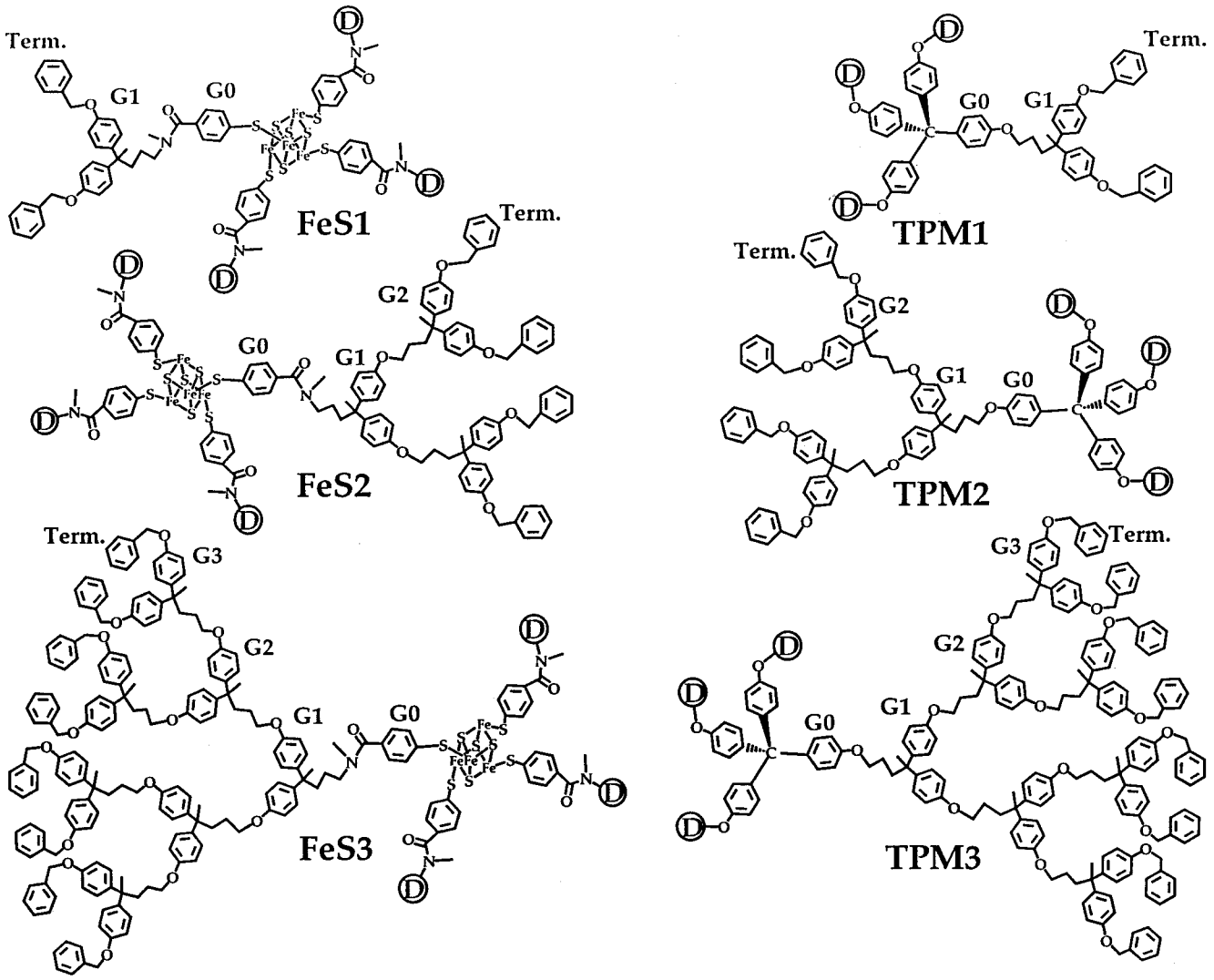

Figure 1. Molecules considered in this study. The FeS type molecules are dianions and are prepared as bis(tetrabutylammonium) salts.

Specifically, dendrimers of generations 1−3 were synthesized that contained either a paramagnetic $[Fe_4S_4(SR)_4]^{2-}$ (FeS) core or a diamagnetic tetraphenylmethane (TPM) core. Both the FeS and TPM dendrimers have similar ligands about the core and a similar symmetry at the core. As a clear, graphical representation of these molecules is difficult, only one of the four dendrons comprising the dendrimer is shown in detail in Figure 1. The other three dendron arms around the core are abbreviated (as a circled D) but have the same structure as the fully drawn dendron. The designations G0, G1 ..., G*n* refer to the aromatic protons at the *n*th branch point (generation) in the molecule. The designation Term. refers to the topologically peripheral C_6H_5 groups. The superscripts A and B merely denote the more upfield and downfield signals, respectively, in the AA′XX′ pattern for the different para-substituted phenyl rings considered. Throughout this paper, the term "generation" will be used to denote a group of repeat units at the same topological branch point within a given dendrimer rather than to refer to the number of branch points in the dendrimer.

The FeS core dendrimers **FeS1**, **FeS2**, and **FeS3** (Figure 1) were available from a previous study.[26] Briefly, their synthesis was accomplished via a ligand exchange of bulky aliphatic thiol ligands in the precursor cluster $(n\text{Bu}_4\text{N})_2[Fe_4S_4(S\text{-}t\text{Bu})_4]$ with 4 equiv of a focally substituted aromatic thiol dendron. Their characterization by NMR, UV−vis spectroscopy, and vapor-phase osmometry was found to be consistent with the structures drawn in Figure 1.

The TPM core dendrimers were prepared by reaction of 4.4 equiv of a focally substituted mesyl dendron[39] with tetrakis(*p*-hydroxylphenyl)methane as described in the Experimental Section. These reactions generally proceeded in very low yields. These low yields monotonically decreased with increasing dendrimer size and most probably reflected the steric difficulty in assembling four dendrons around this core. Such difficulties have been noted previously in other, completely convergent syntheses of dendrimers.[40−44] Nevertheless, these molecules could be obtained, as evidenced by NMR, matrix-assisted laser desorption ionization (MALDI) mass spectrometry, and gel permeation chromatography.

B. Comparison of the Relaxation Behavior of Diamagnetic and Paramagnetic Core Dendrimers. Proton NMR spectra of the aromatic regions of FeS and TPM core dendrimers are shown in Figures 2 and 3, respectively. These resonances have sufficiently different chemical shifts so as to distinguish, to a point, the topologically different generations (e.g. G0, G1, ..., G*n* in Figure 1) within the dendrimer. The benzyl group

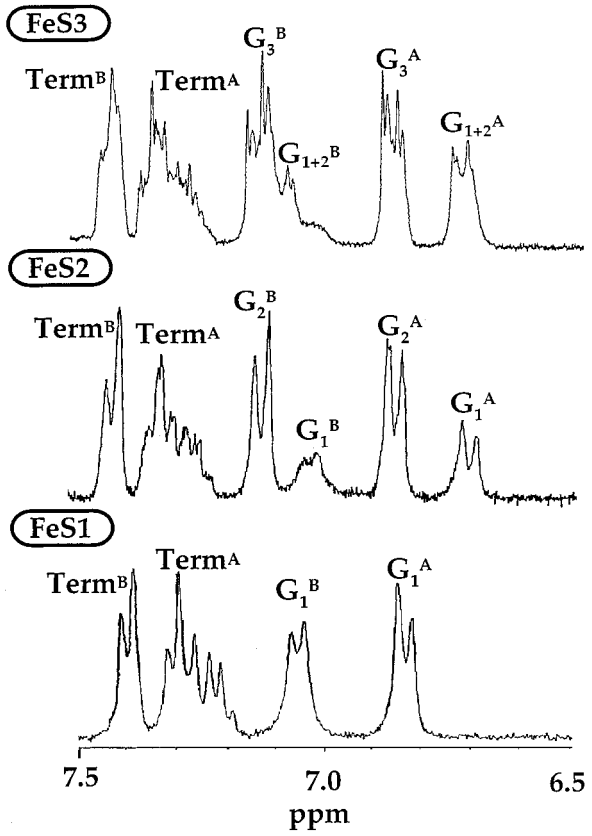

Figure 2. Aromatic regions of the ^{1}H NMR spectra of **FeS1**, **FeS2**, and **FeS3**.

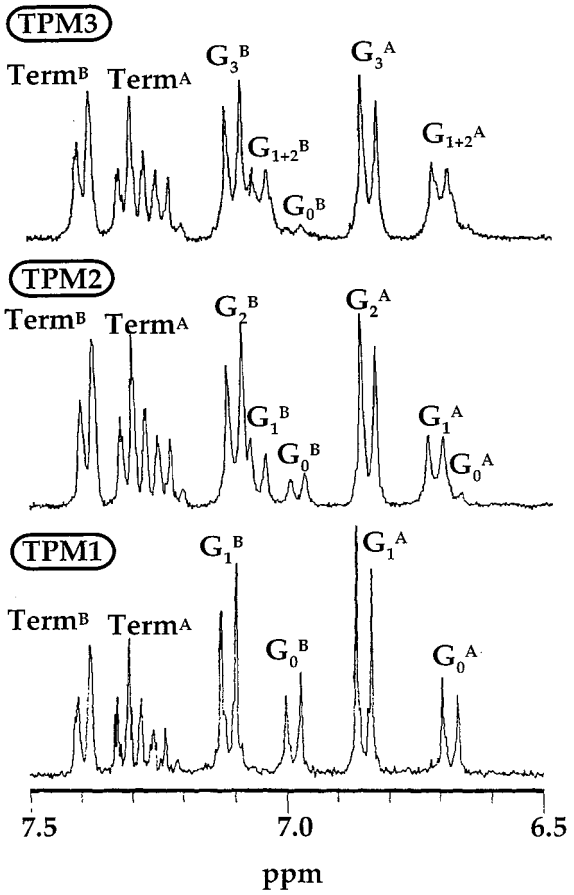

Figure 3. Aromatic regions of the ^{1}H NMR spectra of **TPM1**, **TPM2**, and **TPM3**.

resonance (designated Bn in Figure 4), although not shown in these spectra, was also considered in this study. This resonance appeared as a singlet at 5.0 ppm for all the molecules considered. Other ^{1}H NMR resonances as well as ^{13}C NMR resonances for these molecules did not satisfy this criterion and were not considered further.

The paramagnetic center in the FeS dendrimers, although it resulted in shifting and broadening of the G0 protons, did not dramatically affect the chemical shift or broadness of the other proton signals in the dendrons (Figure 2). The signals were thus assignable to the different generations. Furthermore, this observation indicated a lack of Fermi contact as a mechanism for influencing either the chemical shifts or the T_1 values of these other protons.

The most notable difference in the relaxation data (Figure 4) was the dramatic shortening of T_1 values for the protons in the paramagnetic core (FeS) dendrimers as compared to those in the diamagnetic core (TPM) dendrimers. This shortening is attributed to the direct, through-space interaction of these protons with the core of the dendrimers. This observation leads to the most significant result of this paper—protons in each generation of these dendrimers must approach the core of the molecule closely in space to experience the attenuation in T_1 observed for the FeS dendrimers compared to that of TPM dendrimers. The value of T_1 measured is an average T_1 for the protons in each generation of the molecule. Thus, an attenuated T_1 value due to the presence of a paramagnetic core indicates qualitatively that some of each set of protons approach the core closely on the time scale of the NMR experiment.

This conclusion assumes that spin diffusion (nuclear–nuclear spin exchange) is not important in this case.[45,46] This assumption should be reasonable for two reasons. First, the correlation times for spin diffusion should be too short for molecules of this size in a solution environment. Second, if spin diffusion were operative in shortening the T_1 values of all the protons in the FeS dendrimers, these values should all be the same. While, the T_1 values of the topologically interior protons are similar, the T_1 values of the topologically exterior (e.g. $Term_A$ and $Term_B$) protons are quite different. Relaxation, particularly of the topologically exterior protons, is not due to spin diffusion.

In all of the molecules described here, relaxation is attributed to dipole–dipole (DD) relaxation[47–49] between two nuclei (in both the FeS and TPM dendrimers) and between a nucleus and the unpaired electrons at the core (in only the FeS dendrimers). Other mechanisms for nuclear relaxation such as chemical shift anisotropy and scalar coupling are unlikely to give rise to the trends illustrated here, as these phenomena are generally insignificant in fluid solution and where chemically identical but topologically (more importantly, conformationally) different nuclei are considered. This was also the conclusion of Meltzer et al. in a study of T_1 relaxation of ^{13}C nuclei in another type (PAMAM) of dendrimer structure.[36]

A model of dendrimer conformation in which different generations of the dendrimer are interspersed throughout its structure was supported by atomistic molecular dynamics simulations on these molecules. Figure 5 shows the radial density distribution of the different generations within a model of **FeS3** (in which the iron–sulfur core was represented with a cubane core) averaged over the last 25 ps of a 100-ps molecular dynamics

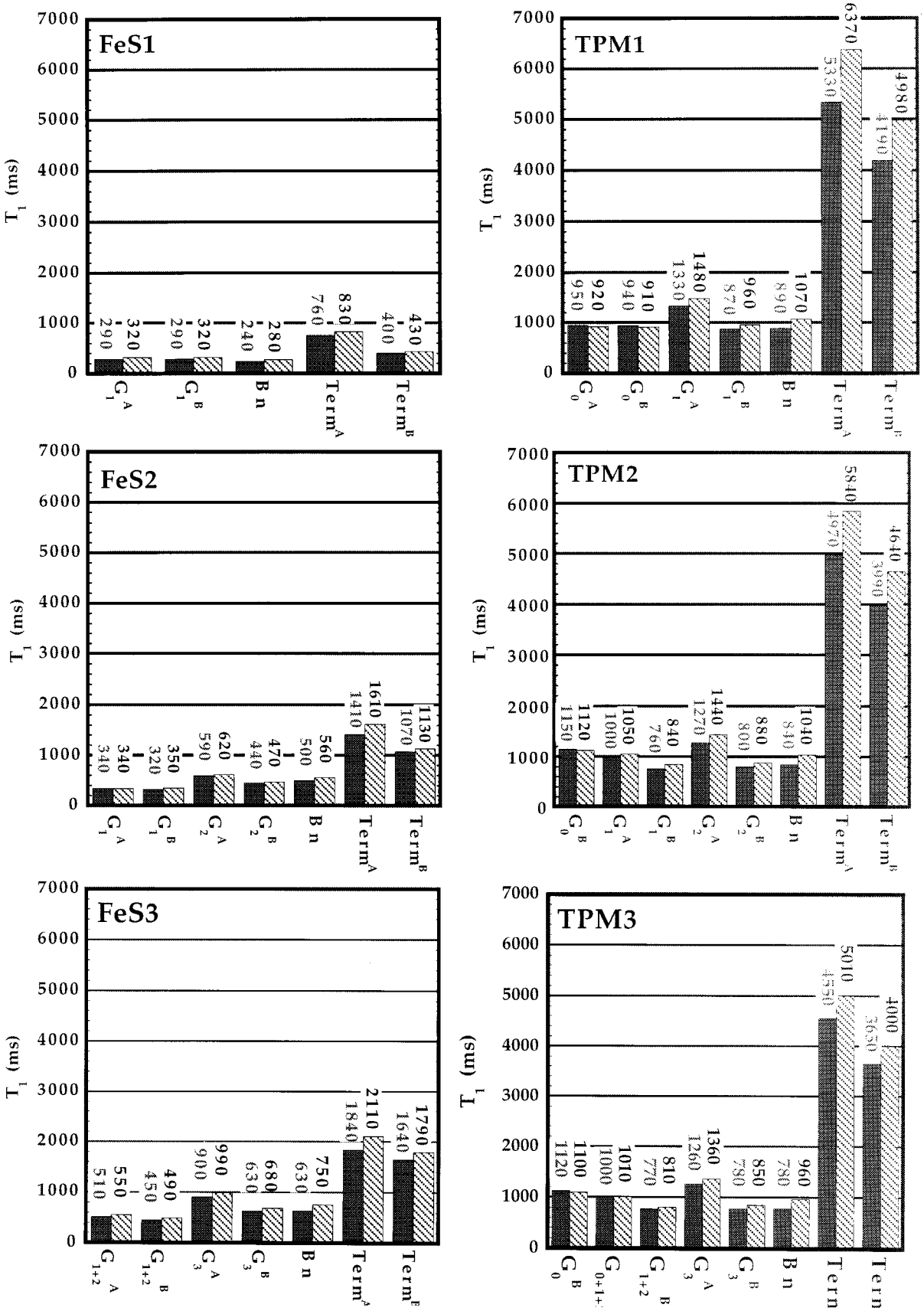

Figure 4. Tabulation of T_1 values at 25 °C (solid bars) and 40 °C (dashed bars).

simulation. The radial density distributions calculated for TPM3 were similar. This simulation depicted a compact, globular dendrimer with a trend in radial densities of each of the different generations that is consistent with the NMR relaxation data. Although this simulation is for a much shorter time scale than that

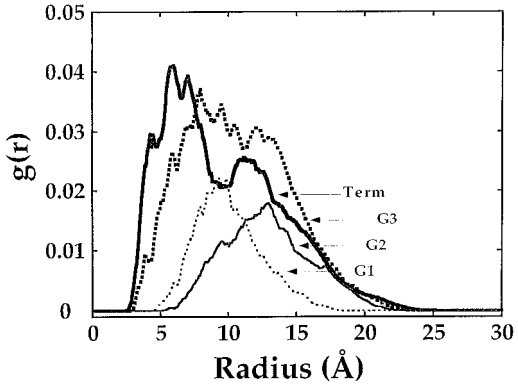

Figure 5. Radial density distribution functions of the generations (as designated in Figure 1) within a model of **FeS3**.

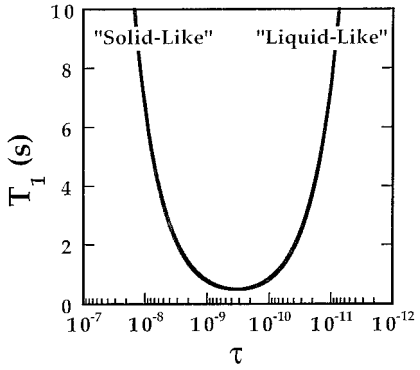

Figure 6. Dependence of T_1 on internuclear correlation time (τ) for two protons separated by 2 Å in a 300.522-MHz magnetic field.[51] This treatment assumes only DD relaxation between the two nuclei and the field and indicates the so-called solid-like and liquid-like regimes for relaxation as a function of internuclear motion.

of the NMR experiment, it illustrates that some of the protons at each generation of the dendrimer can come into close proximity to the core.

C. Relative Conformational Flexibility. The nuclei in the dendrimers studied here all exhibited internuclear motion consistent with the behavior in a liquid-like regime.[47−49] This conclusion was made by considering the change in T_1 values of the nuclei within each molecule as the temperature was slightly elevated. It was not our intention to use temperature to widely vary internuclear correlation time and thus T_1, as it is not clear that one can predict either how the microviscosity within the dendrimer or its conformational manifold might change with temperature. This small perturbation, however, was designed to increase internuclear motion in the dendrimer slightly, thus decreasing the internuclear correlation time. In all cases here, T_1 remained constant or increased with a slight increase in temperature. This behavior is consistent with internuclear correlation times in the liquid-like regime, possibly near the τ versus T_1 minimum.

The trends in T_1 illustrated here reflect more motions than overall rotation of the molecules. To show this, the overall rotational correlation times of **TPM1**, **TPM2**, and **TPM3** were estimated from their average radii as computed from the molecular dynamics simulations described above. Average radii over the molecular dynamics trajectories of 10, 14, and 18 Å were computed for **TPM1**, **TPM2**, and **TPM3**, respectively. These radii were used to estimate the correlation time from the Stokes−Einstein equation

$$\tau_r = \frac{4\pi\eta a^3}{3kT}$$

where η is the viscosity of THF (0.46×10^{-3} (J·s)/m^3 at room temperature),[50] k is Boltzman's constant (1.38×10^{-23} J/K), T is the absolute temperature, and a is the average radius of the dendrimer. This computation lead to overall rotational correlation times of 4.69×10^{-10}, 1.29×10^{-9}, and 2.73×10^{-9} s for **TPM1**, **TPM2**, and **TPM3**, respectively. These times were computed to change by less than 5% between 298 and 313 K assuming no change in solvent viscosity or dendrimer conformation over this temperature range. On the basis of the relationship between T_1 and τ shown in Figure 6,[51] one would expect "solid-like" relaxation behavior if molecular rotation was the only type of motion responsible for DD relaxation. This type of behavior is not observed here, since one would expect a decrease in T_1 with increasing temperature in this regime instead of the observed increase.

The T_1 values of the topologically interior protons in the dendrimers changed very little with a small change in temperature (Figure 4). Many of the differences were within the 5% error attributed to the experiment. The invariance of T_1 with temperature could be attributed to nuclei with a correlation time near the τ versus T_1 minimum. This behavior thus suggests that the interior nuclei in each of the dendrimers are densely packed, limiting the relative amount of high-frequency motion. New avenues for either additional motion or much of an increase in the frequency of motion do not become available with this small increase in temperature for these nuclei.

In contrast, the terminal protons ($Term_A$ and $Term_B$) in both kinds of dendrimers behaved differently from those for the other nuclei. Their T_1 values were longer. Moreover, they exhibited a greater temperature dependence of T_1 over the small range studied. Both of these behaviors are consistent with increased motion of these groups as compared to all others in the molecules. Thus, over the time scale of the NMR experiment, a number of these groups are near the geometric periphery of the molecules, where they are not densely packed and can move more. Molecular dynamics simulations suggest that, at least on a short time scale, this motion is predominantly rapid rotation of these benzene rings.

This type of differential motion between the interior and terminal protons was illustrated by calculating the mean square displacement correlation functions for the atoms at each topologically distinct site in the model of the FeS3 dendrimer considered in Figure 5. Such a graph is shown in Figure 7 for the last 80 ps of the molecular dynamics run performed. A molecular dynamics run of this duration is too short to be used in a quantitative calculation of the correlation times of the various motions contributing to DD relaxation.[52] However, in this short period, one can distinguish very different relative mobilities of groups. Indeed, in Figure 7, the terminal groups in the molecule are predicted to move about much more than any of the other groups.

This relatively higher mobility reflects that of an average terminal group in a given dendrimer. Initially, it might appear that this higher mobility is inconsistent with the notion that terminal groups can be found in the core region of the dendrimer. However, these two average behaviors can exist simultaneously in a den-

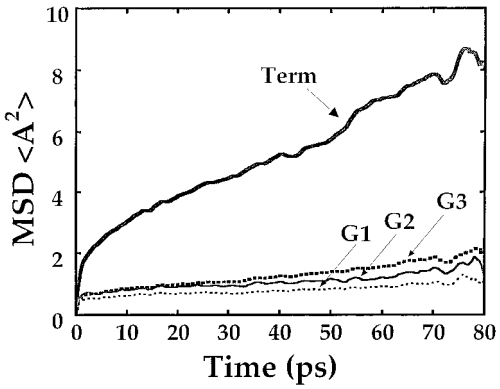

Figure 7. Mean square displacement correlation functions of the generations (as designated in Figure 1) for a model of **FeS3**.

drimer architecture. Some of the terminal groups can be found close to the dendrimer core, resulting in a decrease in their average T_1 value when this core is paramagnetic. A number of the terminal groups, however, reside at the molecular periphery and are thus more mobile than the others. Over the course of a molecular dynamics trajectory, on average, 25 of the 32 terminal groups were found at the geometric periphery of the model of **FeS3** and 3 of the 32 terminal groups were found within 6 Å of the molecular core.

Conclusions

Dendrimers with paramagnetic cores offer a handle for qualitatively evaluating some general conformational features of dendrimers. Specifically, the attenuation of T_1 values for protons in paramagnetic core dendrimers as compared to those in similar diamagnetic core dendrimers indicates a dendrimer structure for dendrimers up to generation 3 containing floppy subunits in which, on average, the protons in each different generation of a dendrimer approach the core of the molecule closely in space. This conclusion agrees with the computed radial density distributions of these different generations that could be calculated from molecular dynamics simulations.

These T_1 values as well as their change with a slight change in temperature also suggest liquid-like mobility, most particularly for the terminal groups on the dendrimer. This observation is consistent with a geometric distribution of terminal groups in which many are at the geometric exterior of the dendrimers and are thus capable of more segmental motion. This conclusion is supported by the computed mean square displacement correlation functions for the different generations that could be calculated from molecular dynamics simulations.

These observations support a model of a dendrimer with a compact interior and a more mobile exterior. This packed interior, however, does not find the topologically most central groups exclusively at the geometric center of the molecule. Rather, over the time scale of the experiment, some members of each of the different generations within the dendrimer establish a position close to the core of the molecule. These conclusions are consistent with recent computational predictions about dendrimer conformation[53−57] and help to provide a general physical picture for dendrimer conformation and flexibility that, to date, has had only modest experimental evidence to support it.

Experimental Section

Synthesis—General Considerations. All starting compounds were purchased from Aldrich Chemical and were used without further purification unless otherwise noted. Acetone was dried from molecular sieves. Methanol was distilled from magnesium methoxide. Chloroform and methylene chloride were distilled from calcium hydride. Tetrahydrofuran was distilled from sodium benzophenone ketyl. All reactions were run under a nitrogen atmosphere. Flash chromatography was run on 230−400 mesh silica gel (Merck). Nuclear magnetic resonance characterization was performed at 300 MHz (^{1}H) or 75 MHz (^{13}C) on a GE-NMR system. High-resolution mass spectrometry was performed at the NC State mass spectrometry facility. Gel permeation chromatography was performed using three Jordi polystyrene/divinylbenzene columns in series with pore sizes of 10 000, 1000, and 500 Å, respectively, using simultaneous refractive index and ultraviolet absorption (254 nm) detection.

Tetrakis(*p*-hydroxylphenyl)methane. To a solution of tetrakis(*p*-bromophenyl)methane[58] (575 mg, 0.904 mmol) in 180 mL of dry THF was added *tert*-butyllithium (5.0 mL of a 1.4 M solution in hexanes, 7.23 mmol) dropwise at −78 °C under nitrogen. This mixture was stirred for 1 h at −78 °C, and then tetramethylethylenediamine (420 mg, 3.62 mmol) was added. After an additional 1 h at −78 °C, trimethylborate (2.76 g, 26.59 mmol) was added dropwise and the mixture was stirred for 8 h with gradual warming to room temperature. Then the mixture was cooled to 0 °C and treated with acetic acid (2.40 g, 39.89 mmol) and hydrogen peroxide (3.60 mL of 30% aqueous solution, 31.91 mmol). After it was warmed to room temperature, the mixture was stirred for 10 h, diluted with ether (200 mL), and treated with saturated ferrous ammonium sulfate (90 mL). The aqueous phase was extracted with ether (2 × 50 mL), and the combined organic layers were washed sequentially with saturated sodium bicarbonate (50 mL) and brine (50 mL), dried over magnesium sulfate, filtered, and concentrated with a rotary evaporator. The residue was purified by flash chromatography on silica gel, eluting with 3:2 ether/petroleum ether to give tetrakis(*p*-hydroxylphenyl)-methane as a white powder: yield 40% (140 mg); R_f = 0.21 (4:1 ether/petroleum ether); ^{1}H NMR (d_6-acetone) δ 6.70 (d, 8 H, J = 8.7 Hz), 6.94 (d, 8 H, J = 8.7 Hz), 8.24 (s, 4 H, Ar−OH; D_2O exchange); ^{13}C NMR (d_6-acetone) δ 62.24, 114.08, 132.15, 139.10, 155.39. HRFAB: Calcd for $C_{25}H_{20}O_4$, 384.1362; found, 384.1349.

General Procedure for Preparation of TPM Core Dendrimers. Dendritic mesylates ([G-1]-OMs, [G-2]-OMs, and [G-3]-OMs) were prepared as described previously.[39] A mixture of the dendritic mesylate (4.4 equiv), tetrakis(*p*-hydroxylphenyl)methane (1.0 equiv), anhydrous potassium carbonate (12 equiv), and 18-crown-6 (0.5 equiv) in dry acetone (ca. 0.2 mmol of phenol/mL of acetone) was heated at reflux and stirred vigorously under nitrogen for 72 h. The mixture was cooled, evaporated, and partitioned between methylene chloride and water. The aqueous layer was extracted with methylene chloride (2×). The combined organic layers were washed with brine, dried over magnesium sulfate, filtered, and concentrated with a rotary evaporator. The residue was purified by flash chromatography on silica gel, eluting with 1:1 hexanes or petroleum ether/methylene chloride, increasing to methylene chloride and then to 1:20 ether/methylene chloride. Fractions were collected and further purified by fractional precipitation with methylene chloride/ether/petroleum ether.

TPM1: yield 51% (400 mg) as a white powder; ^{1}H NMR ($CDCl_3$) δ 1.55−1.62 (m, 20 H), 2.19 (m, 8 H), 3.85 (t, 8 H, J = 5.9 Hz), 5.02 (s, 16 H), 6.72 (d, 8 H, J = 8.8 Hz), 6.88 (d, 16 H, J = 8.8 Hz), 7.02 (d, 8 H, J = 8.8 Hz), 7.12 (d, 16 H, J = 8.8 Hz), 7.31−7.44 (m, 40 H); ^{13}C NMR ($CDCl_3$) δ 25.00, 27.96, 38.37, 44.83, 62.22, 68.24, 70.01, 113.05, 114.19, 127.48, 127.86, 128.27, 128.52, 131.96, 137.20, 139.64, 142.01, 156.733, 156.86. HRFAB: Calcd for $C_{149}H_{140}O_{12}$, 2121.0345; found, 2121.1311. GPC: M_n 3250 vs PS, PDI = 1.01.

TPM2: yield 18% (260 mg) as a white powder; ^{1}H NMR ($CDCl_3$) δ 1.25−1.30 (m, 8 H), 1.53−1.64 (m, 52 H), 2.20−2.22 (m, 24 H), 3.88 (apparent t, 24 H), 5.05 (s, 32 H), 6.64 (apparent d, 8 H), 6.77 (d, J = 8.7 Hz, 16 H), 6.90 (d, J = 8.1 Hz, 32 H), 7.05 (d, J = 8.7 Hz, 8 H), 7.12 (apparent d, 16 H), 7.15 (d, J = 8.7 Hz, 32 H), 7.32−7.46 (m, 80 H); ^{13}C NMR ($CDCl_3$) δ 25.07, 28.01, 29.74, 38.41, 44.87, 68.35, 70.05, 113.83, 114.24, 127.54, 127.92, 128.32, 128.57, 131.99, 137.25, 141.69, 142.08, 156.77, 156.92. MALDI-TOF-MS: Calcd for $C_{341}H_{332}O_{28}$ (M + Na), 4901.4; found, 4903.4. GPC: M_n 4450 vs PS, PDI = 1.02.

TPM3: yield 7% (18.5 mg) as a white powder; ^{1}H NMR (d_8-THF) δ 1.30−1.72 (m, 140 H), 2.18 (m, 56 H), 3.80 (m, 56 H), 5.00 (s, 64 H), 6.70 (d, J = 8.7 Hz, 56 H), 6.84 (d, J = 8.7 Hz, 64 H), 6.98 (apparent d, 8 H), 7.05 (d, J = 8.7 Hz, 48 H), 7.09 (d, J = 9 Hz, 64 H), 7.22−7.32 (m, 96 H), 7.37−7.4 (m, 64 H); ^{13}C NMR (d_8-THF) δ 26.11, 28.67, 39.58, 45.88, 69.28, 70.80, 114.77, 115.16, 128.41, 128.61, 129.31, 138.99, 142.79, 143.17, 158.20, 158.36. MALDI-TOF-MS: Calcd for $C_{725}H_{716}O_{60}$, 10 389.6; found, 10 386.7. GPC: M_n 9350 vs PS, PDI = 1.03.

Measurement of T_1 Values. T_1 values were measured using a standard 180−τ−90 inversion recovery pulse sequence. Tetrahydrofuran-d_8 was employed as the solvent, as all six of the dendrimers under consideration were soluble in this solvent. The solvent was freshly distilled from sodium benzophenone ketyl before use, and the samples were prepared in an inert atmosphere glovebox to avoid paramagnetic impurities including oxygen. Dilute (10^{-4} M) solutions were employed to avoid intermolecular relaxation effects between dendrimers. At higher concentrations of dendrimer, smaller T_1 values were obtained, indicative of some intermolecular relaxation at these higher concentrations. Variable delays (τ) were selected to span a range sufficient to probe relaxation up to five times the T_1 values of all of the protons under consideration. A minimum of 10 τ values were employed. Integrals of the proton signals versus τ were plotted and fit to a three-parameter fit using the procedure of Levy and Peat.[59] A 5% standard error in integration was found to be the major source of error in the measurement.

Molecular Dynamics Simulations. All simulations were performed on a Silicon Graphics INDIGO2 R4400 workstation using the BIOSYM modules INSIGHTII and DISCOVER (3.0.0). The all-atom 'consistent valence force field' (CVFF) which includes explicit hydrogens was used for molecular mechanics and molecular dynamics. Atoms were treated as interacting points held together by potential energy terms. The bonded interactions considered were bond stretching, angle bending, torsion, and out-of-plane bending. Nonbonded van der Waals interactions were treated with a 12−6 Lennard-Jones function, and electrostatic interactions were calculated with a non-distance-dependent dielectric constant. The Verlet velocity algorithm was used for integrating equations of motion during molecular dynamics.

A simulated annealing protocol was implemented to generate a reasonable minimum energy structure on which to collect structural data. Bonds were constrained to their equilibrium distances using the RATTLE algorithm (velocity version of SHAKE), permitting the use of a 2-fs time step.[60,61] A nonbond cutoff limit of 9.5 Å was used as well.

The simulated annealing procedure involved 100 ps of high-temperature dynamics at 600 K to ensure adequate sampling of the potential energy surface. Subsequently, the system was cooled to 50 K at a rate of 20 K/ps and minimized to a maximum derivative less than 0.001 kcal mol^{-1} Å^{-1}. This structure was subjected to 20 ps of low-temperature dynamics at 273 K to attain dynamic equilibrium and subsequently sampled for an additional 80 ps. Trajectory coordinates were recorded every 100 fs. Radial density distribution functions (RDFs) and molecular radii were averaged over the last 25 ps of this trajectory. Mean square displacement (MSD) correlation functions were tabulated for the last 80 ps of this trajectory. For the FeS dendrimer series, the iron−sulfur core was replaced by cubane to fulfill the valence requirements of the force field atom types.

Acknowledgment. We thank Professor Ed Stejskal for helpful advice and comments, particularly a lucid explanation of the mechanism for dipole−dipole relaxation. This research was supported by the Air Force Office of Scientific Research MURI program in Nanoscale Chemistry and by the National Science Foundation (CAREER Award, DMR-9600138). Mass spectra were obtained at the Mass Spectrometry Laboratory for Biotechnology. Partial funding for the facility is from NSF Grant 94-2.

References and Notes

(1) Wallimann, P.; Seiler, P.; Diederich, F. *Helv. Chim. Acta* **1996**, *79*, 779−788.
(2) Aoi, K.; Itoh, K.; Okada, M. *Macromolecules* **1995**, *28*, 5391−5393.
(3) Turro, N. J.; Barton, J. K.; Tomalia, D. A. *Acc. Chem. Res* **1991**, *24*, 332−340.
(4) Watanabe, S.; Regen, S. L. *J. Am. Chem. Soc.* **1994**, *116*, 8855−8856.
(5) Wells, M.; Crooks, R. M. *J. Am. Chem. Soc.* **1996**, *118*, 3988−3989.
(6) Bar, G.; Rubin, S.; Cutts, R. W.; Taylor, T. N.; Zawodzinski, T. A. *Langmuir* **1996**, *12*, 1172−1179.
(7) Saville, P. M.; Reynolds, P. A.; White, J. W.; Hawker, C. J.; Fréchet, J. M. J.; Wooley, K. L.; Penfold, J.; Webster, J. R. P. *J. Phys. Chem.* **1995**, *99*, 8283−8289.
(8) Brunner, H. *J. Organomet. Chem.* **1995**, *500*, 39−46.
(9) Chang, H.-T.; Chen, C.-T.; Kondo, T.; Suizdak, G.; Sharpless, K. B. *Angew. Chem., Int. Ed. Engl.* **1996**, *35*, 182−186.
(10) Jansen, J. F. G. A.; Meijer, E. W.; de Branbander-Van den Berg, E. M. M. *J. Am. Chem. Soc.* **1995**, *117*, 4417−4418.
(11) Jansen, J. F. G. A.; Janssen, R. A. J.; de Branbander-Van den Berg, E. M. M.; Meijer, E. W. *Adv. Mater.* **1995**, *7*, 561−564.
(12) Hawker, C. J.; Farrington, P. J.; Mackay, M. E.; Wooley, K. L.; Fréchet, J. M. J. *J. Am. Chem. Soc.* **1995**, *117*, 4409−4410.
(13) Mourey, T. H.; Turner, S. R.; Rubinstein, M.; Fréchet, J. M. J.; Hawker, C. J.; Wooley, K. L. *Macromolecules* **1992**, *25*, 2401−2406.
(14) Percec, V.; Chu, P.; Ungar, G.; Zhou, J. *J. Am. Chem. Soc.* **1995**, *117*, 11441−11454.
(15) Hawker, C. J.; Wooley, K. L.; Fréchet, J. M. J. *J. Am. Chem. Soc.* **1993**, *115*, 4375−4376.
(16) Dandliker, P. J.; Diederich, F.; Gross, M.; Knobler, C. B.; Louati, A.; Sanford, E. M. *Angew. Chem., Int. Ed. Engl.* **1994**, *33*, 1739−1741.
(17) Dandliker, P. J.; Diederich, F.; Gisselbrecht, J.-P.; Louati, A.; Gross, M. *Angew. Chem., Int. Ed. Engl.* **1995**, *34*, 2725−2727.
(18) Janssen, R. A. J.; Jansen, J. F. G. A.; van Haare, J. A. E. H.; Meijer, E. W. *Adv. Mater.* **1996**, *8*, 494−496.
(19) Sadamoto, R.; Tomioka, N.; Aida, T. *J. Am. Chem. Soc.* **1996**, *118*, 3978−3979.
(20) Tomoyose, Y.; Jiang, D.-L.; Jin, R.-H.; Aida, T.; Yamashita, T.; Horie, K.; Yashima, E.; Okamoto, Y. *Macromolecules* **1996**, *29*, 5236−5238.
(21) Ihre, H.; Hult, A.; Söderlind, E. *J. Am. Chem. Soc.* **1996**, *118*, 6388−6395.
(22) Wiener, E. C.; Auteri, F. P.; Chen, J. W.; Brechbiel, M. W.; Gansow, O. A.; Schneider, D. S.; Belford, R. L.; Clarkson, R. B.; Lauterbur, P. C. *J. Am. Chem. Soc.* **1996**, *118*, 7774−7782.
(23) Ottaviani, M. F.; Montalti, F.; Romanelli, M.; Turro, N. J.; Tomalia, D. A. *J. Phys. Chem.* **1996**, *100*, 11033−11042.
(24) Ottaviani, M. F.; Cossu, E.; Turro, N. J.; Tomalia, D. A. *J. Am. Chem. Soc.* **1995**, *117*, 4387−4398.
(25) Ottaviani, M. F.; Bossman, S. H.; Turro, N. J.; Tomalia, D. A. *J. Am. Chem. Soc.* **1994**, *116*, 661−671.
(26) Gorman, C. B.; Parkhurst, B. L.; Chen, K.-Y.; Su, W. Y. *J. Am. Chem. Soc.* **1997**, *119*, 1141−1142.
(27) González-Moraga, G. in *Cluster Chemistry*; Springer-Verlag: New York, 1993; pp 278−295.
(28) Babini, E.; Bertini, I.; Borsari, M.; Capozzi, F.; Dikiy, A.; Eltis, L. D.; Luchinat, C. *J. Am. Chem. Soc.* **1996**, *118*, 75−80.
(29) Agarwal, A.; Li, D.; Cowan, J. A. *J. Am. Chem. Soc.* **1996**, *118*, 927−928.
(30) Averill, B. A.; Herskovitz, T.; Holm, R. H.; Ibers, J. A. *J. Am. Chem. Soc.* **1973**, *95*, 3523−3534.

(31) Que, Jr.; L., Bobrik, M. A.; Ibers, J. A.; Holm, R. H. *J. Am. Chem. Soc.* **1974**, *96*, 4168−4177.
(32) DePamphilis, B. V.; Averill, B. A.; Herskovitz, T.; Que, Jr.; L., Holm, R. H. *J. Am. Chem. Soc.* **1974**, *96*, 4159−4167.
(33) Holm, R. H.; Phillips, W. D.; Averill, B. A.; Mayerle, J. J.; Herskovitz, T. *J. Am. Chem. Soc.* **1974**, *96*, 2109−2117.
(34) Holm, R. H. *Acc. Chem. Res* **1977**, *10*, 427−434.
(35) Herskovitz, T.; Averill, B. A.; Holm, R. H.; Ibers, J. A.; Phillips, W. D.; Weiher, J. F. *Proc. Natl. Acad. Sci.* **1972**, *69*, 2437−2441.
(36) Meltzer, A. D.; Tirrell, D. A.; Jones, A. A.; Inglefield, P. T.; Hedstrand, D. M.; Tomalia, D. A. *Macromolecules* **1992**, *25*, 4541−4548.
(37) Meltzer, A. D.; Tirrell, D. A.; Jones, A. A.; Inglefield, P. T. *Macromolecules* **1992**, *25*, 4549−4552.
(38) Wooley, K. L.; Klug, C. A.; Tasaki, K.; Schaefer, J. *J. Am. Chem. Soc.* **1997**, *119*, 53−58.
(39) Chen, K.-Y.; Gorman, C. B. *J. Org. Chem.* **1996**, *61*, 9229−9235.
(40) Kawaguchi, T.; Walker, K. L.; Wilkins, C. L.; Moore, J. S. *J. Am. Chem. Soc.* **1995**, *117*, 2159−2165.
(41) Xu, Z.; Kahr, M.; Walker, K. L.; Wilkins, C. L.; Moore, J. S. *J. Am. Chem. Soc.* **1994**, *116*, 4537−4550.
(42) Hawker, C. J.; Fréchet, J. M. J. *J. Am. Chem. Soc.* **1990**, *112*, 7638−7647.
(43) Hawker, C. J.; Fréchet, J. M. J. *J. Am. Chem. Soc.* **1992**, *114*, 8405−8413.
(44) Wooley, K. L.; Hawker, C. J.; Fréchet, J. M. J. *J. Am. Chem. Soc.* **1991**, *113*, 4252−4261.
(45) Kalk, A.; Berendsen, H. J. C. *J. Magn. Reson.* **1976**, *24*, 343−366.
(46) For a recent example of spin diffusion in the solid state, see: Eckman, R. R.; Henrichs, P. M.; Peacock, A. J. *Macromolecules* **1997**, *30*, 2474−2481.
(47) Bovey, F. A.; Jelinski, L.; Mirau, P. A. In *Nuclear Magnetic Resonance Spectroscopy*, 2nd ed.; Academic Press: New York, 1988; Chapter 5.
(48) Noggle, J. H.; Schirmer, R. E. In *The Nuclear Overhauser Effect. Chemical Applications*; Academic Press: New York, 1971; Chapter 2.
(49) Sanders, J. K. M.; Hunter, B. K. *Modern NMR Spectroscopy: A Guide for Chemists*, 2nd ed.; Oxford University Press: New York, 1993; pp 161−163.
(50) Snyder, L. R. In *Introduction to Modern Liquid Chromatography*, 2nd ed.; John Wiley and Sons, Inc.: New York, 1979; p 248.
(51) This curve was calculated at an internuclear separation of 2 Å using a program employing the GAMMA function library. This library is available from (http://gamma.magnet.fsu.edu/download/packages/). The program upon which this calculation was based is available from (http://gamma1.magnet.fsu.edu/~gamma/htmldox/relax/dipolar.fm45.html). The literature reference for these calculations is: Smith, S. A.; Levante, T. O.; Meier, B. H.; Ernst, R. R. *J. Magn. Reson.* **1994**, *106a*, 75−105.
(52) This power spectrum can be used to compute T_1 assuming a DD relaxation mechanism. However, this requires a molecular dynamics simulation on the order of 100 ns to obtain a spectrum at the relevant frequencies. Such a computation has been performed recently for a small cyclic oligopeptide: Bremi, T.; Brüschweiler, R.; Ernst, R. R. *J. Am. Chem. Soc.* **1997**, *119*, 4272−4284.
(53) Chen, Z. Y.; Cui, S.-M. *Macromolecules* **1996**, *29*, 7943−7952.
(54) Forni, A.; Ganazzoli, F.; Vacatello, M. *Macromolecules* **1996**, *29*, 2994−2999.
(55) Mansfield, M. L.; Klushin, L. I. *J. Phys. Chem.* **1992**, *96*, 3994−3998.
(56) Mansfield, M. L.; Klushin, L. I. *Macromolecules* **1993**, *26*, 4262−4268.
(57) Murat, M.; Grest, G. S. *Macromolecules* **1996**, *29*, 1278−1285.
(58) Grimm, M.; Kriste, B.; Kurreck, H. *Angew. Chem., Int. Ed. Engl.* **1986**, *25*, 1097−1098.
(59) Levy, G. C.; Peat, I. R. *J. Magn. Reson.* **1975**, *18*, 500−521.
(60) Lamy, A.; Smith, J. C. *J. Am. Chem. Soc.* **1996**, *118*, 7326−7328.
(61) Wilson, M. A.; Pohorille, A. *J. Am. Chem. Soc.* **1996**, *118*, 6580−6587.

MA9714979